



Proceedings of the Sixth International Conference on  
Railway Technology: Research, Development and Maintenance  
Edited by: J. Pombo  
Civil-Comp Conferences, Volume 7, Paper 14.3  
Civil-Comp Press, Edinburgh, United Kingdom, 2024  
ISSN: 2753-3239, doi: 10.4203/ccc.7.14.3  
©Civil-Comp Ltd, Edinburgh, UK, 2024

# A Power Electronic Transformer for Rail Vehicles Based on SiC

J. Qu, Y. Zhang, X. Gao, J. Ma and Y. Lei

State Key Laboratory of High-speed Maglev Transportation  
Technology, CRRC QINGDAO SIFANG CO., LTD  
China

## Abstract

In order to realize the miniaturization and weight reduction of the traction drive system of rail vehicles and reduce the motor current distortion caused by the low switching frequency of the traditional converter during high-speed operation of the vehicle, an integrated converter consisting of a power electronic transformer and a sine wave traction inverter based on silicon carbide (SiC) is proposed. The system implementation scheme based on silicon carbide MOSFETs, the design scheme of high-frequency, high-power and high-insulation voltage-resistant magnetic isolation, and the communication design scheme of low-latency system are given, and the input and output characteristics of the system are analyzed by simulation. The results show that the total harmonic distortion rate of the input current is less than 1 %, the power factor is greater than 0.99, and the output voltage total harmonic distortion rate is less than 3.50% when the rated power is 3.25 MVA. The system efficiency is greater than 97.5%, which is higher than the efficiency of the traditional traction drive system by 3 % ~ 5%.

**Keywords:** silicon carbide, power electronic transformer, sine wave traction inverter, resonant converter, soft switching, power electronic.

## 1 Introduction

The future development of high-speed rail vehicles focuses on the comprehensive improvement of technical indicators such as speed, efficiency, energy conservation, environmental protection, and economy. Higher speed and more intelligence are the

two main directions for the future development of high-speed rail in China. Traction transmission technology is one of the core technologies of railway locomotives and vehicles. Although many host factories in China adopt different technical routes in the design of traction transmission systems, they are basically composed of power frequency traction transformers and traction converters. Due to the low operating frequency of the power frequency traction transformer, its volume and weight are relatively large, for example, the traction transformer of the Fuxing high-speed train reaches 6.4 tons [1]. The operating power of high-speed trains is increasing, and the proportion of higher capacity power frequency transformers in the weight of the entire vehicle is becoming more prominent, which limits the demand for vehicle lightweighting. Due to the technical characteristics of silicon (Si) IGBT, traditional traction converters have limited room for improvement in lightweight and energy-saving performance. At the same time, traditional silicon converters have a low switching frequency during high-speed vehicle operation, which leads to severe distortion of motor current. Railway locomotives and vehicles urgently need to adopt new technologies to promote the development of traction transmission technology and achieve lightweight and miniaturization of traction systems.

SiC technology will break through the performance limits of existing Si technology in three directions: higher blocking voltage, higher operating temperature, and higher switching speed. Compared to Si devices, SiC devices can reduce switching losses by 70% at the same switching voltage change rate ( $dv/dt$ ). The use of SiC devices in traction converters can reduce the volume and weight of the cooling system due to their low loss characteristics, and their high switching frequency characteristics can reduce the volume and weight of passive devices, achieving energy-saving and lightweight of the entire traction system [2,3].

Power electronic transformers generally refer to new types of power electronic equipment that have the functions of traditional power frequency AC transformers, but are not limited to, achieved through power electronic technology and high-frequency transformers. Power electronic transformers are generally used in medium, high voltage, and high-power situations, and can replace traditional power frequency transformers. The application of power electronic transformers is currently mainly concentrated in onboard converter systems for electric locomotive traction, smart grids/energy internet, and distributed renewable energy generation grid connected systems [4,5].

In the application of rail vehicle inverter systems, ABB successfully applied a power electronic transformer to engineering maintenance of electric locomotives in 2011. The power electronic transformer consists of 8 cascaded units based on Si devices, with an output power of 1.2 MVA and a switching frequency of 1.75 kHz. Compared with traditional transformers, it reduces weight by 54%. If SiC devices are used in power electronic transformers, the working frequency of the transformer can be further increased, the volume and weight of the transformer can be reduced, and the goal of lightweight, miniaturization, energy conservation and emission reduction can be achieved [6,7].

This article will apply cascaded multilevel technology and high-frequency resonant soft switching technology to construct an integrated system of electronic power transformer and sine wave traction inverter based on low-voltage SiC devices, in order

to significantly improve system operation efficiency and power density, reduce the volume and weight of traction transmission system.

## 2 Topology Of An Integrated Inverter System

The integrated converter system is shown in Figure 1, which includes 52 identical basic power subunits. This integrated converter system can independently drive 4 traction motors, with a line voltage of 2750 V and a line current of 155 A. The integrated inverter system provides four sets of three-phase 380V AC auxiliary power supplies simultaneously, with each having a rated output power of 50 kVA. In summary, the total load power is 3.16 MVA. Assuming that the efficiency of the integrated converter is 97.50%, the system input power is 3.25 MVA.

The rated voltage of China railway traction contact grid is 25 kV, while the current voltage level of mainstream SiC power devices is 1.2 kV. Considering the influence of certain voltage margin and duty cycle, a modular structure is adopted to achieve series voltage division on the high-voltage input side. A basic power subunit implemented using SiC devices is shown in Figure 2. The intermediate stage DC/DC converter adopts a CLLC resonant converter topology to achieve electrical isolation between the traction grid and the train. Energy can be transmitted in both directions and operates at 150 kHz to significantly reduce the volume and weight of the isolated magnetic unit.

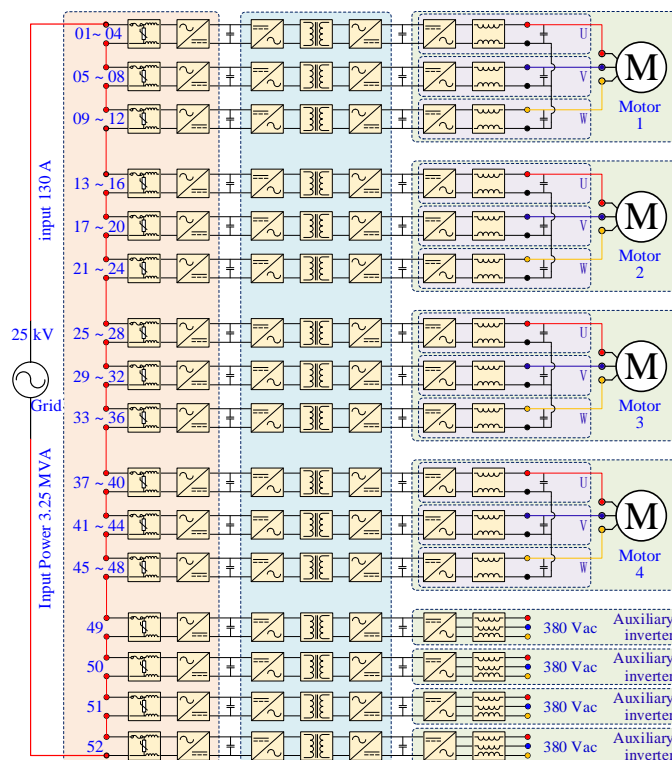


Figure 1: Structure of the integrated converter system

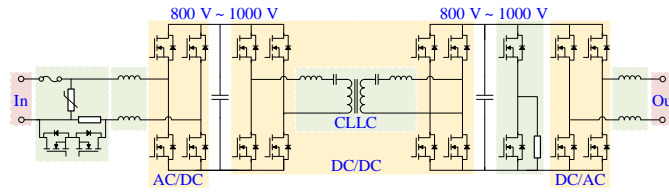
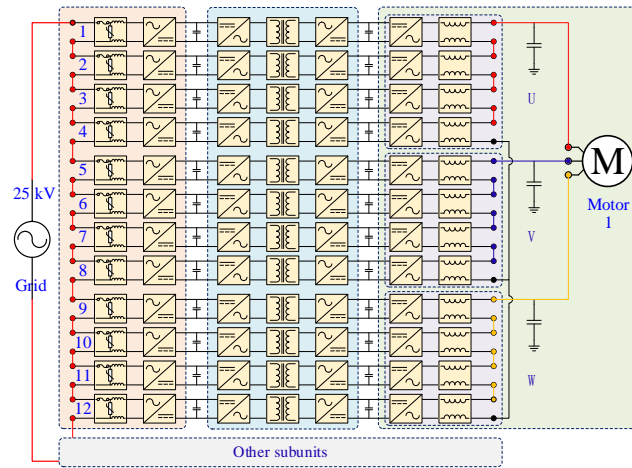
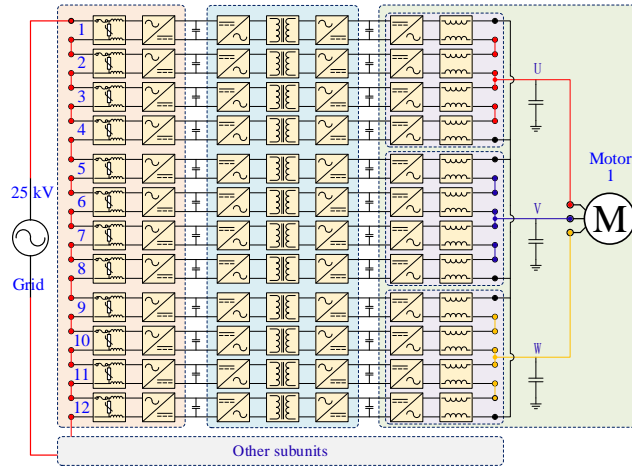


Figure 2: Structure of the basic power subunit



(a) The three-phase four stage cascaded inverter



(b) The three-phase paralleled two stage cascaded inverter

Figure 3: Structure of the cascaded inverter

Each traction motor is independently controlled by a cascaded multi-level inverter scheme consisting of 12 basic power subunits (shaft control mode), which can effectively improve adhesion utilization and can be used to drive permanent magnet motors. There are two cascaded inverter implementation schemes for driving three-phase motors. The first one is a three-phase four stage cascaded inverter scheme as shown in Figure 3(a), which uses four inverter units per phase to form a four stage cascaded inverter that can be applied to higher voltage level motors in the future. A parallel two-stage cascade scheme is adopted, as shown in Figure 3(b). At this time, the on state loss is 25% of the four stage cascade scheme. However, during the rated

power operation of three-phase motors, the DC bus voltage of the basic power unit needs to be greater than 972 V, and it is necessary to optimize the DC bus to reduce parasitic inductance. There is a long connecting cable between the inverter and the motor. In order to reduce the transient voltage spikes caused by the high switching speed characteristics of SiC on the long cable and reduce the risk of insulation voltage resistance of the motor, this design is equipped with an LC filter at the three-phase output end.

### 3 Control Strategy For Integrated Converter

The integrated converter input is directly connected to the traction grid, requiring bidirectional energy flow and operating at a unit power factor. The simulation results of a single-phase 52 stage cascaded PWM rectifier are shown in Figure 4, using a unipolar frequency doubling carrier phase shift modulation method. The switching frequency of the basic power subunit is 10 kHz, the grid voltage is 25 kV, the DC voltage is  $41.60 \pm 4.25$  kV, and the power is 3.25 MW. At this time, the total harmonic distortion rate (THD) of the grid input current is 0.22 %, and the input power factor is 0.99. In the 52 level cascaded multilevel rectification mode, the equivalent switching frequency is  $52^2$  times that of each cascaded rectifier unit, which is 27.04 MHz. This can significantly reduce the inductance of the input filter and reduce its volume, weight, and power loss.

Using the third harmonic injection PWM modulation method, with a switching frequency of 30 kHz, a DC bus voltage of 1000 V, and a modulation ratio of 0.9734, the simulation results of the output voltage of the three-phase parallel two-stage cascade inverter are shown in Figure 5. At this time, the output line voltage is 2749 V, and the output current is 154.4 A. The output line voltage THD is 0.76%, and the main harmonic component is located at the frequency of 240 kHz (8 times the switching frequency). The cut-off frequency of the output filter is 64.97 kHz, where the equivalent filtering inductance 10  $\mu$ H and the equivalent filtering capacitance 0.6  $\mu$ F.

The switching frequency of the CLLC resonant converter in this design is fixed at the resonant frequency (150 kHz), and the output voltage of the front-end AC/DC converter is adjusted to meet the requirements of the post-stage DC/AC inverter. When the ratio of the isolation transformer is  $n=1.0$ , the voltage gain curve under different switching frequencies and load conditions is shown in Figure 6, where the resonant inductance is 5.98  $\mu$ H, the resonant capacitor is 188.17 nF, and the resonant frequency is 150 kHz.

To reduce the transient overcurrent during startup under rated load, the CLLC resonant converter is set to a switching frequency of 300 kHz during startup and linearly decreases to the rated switching frequency of 150 kHz within 50 ms. The simulation results of the output voltage during the transient startup process are shown in Figure 7, and there is no overshoot of the output voltage during the startup process (0-50 ms).

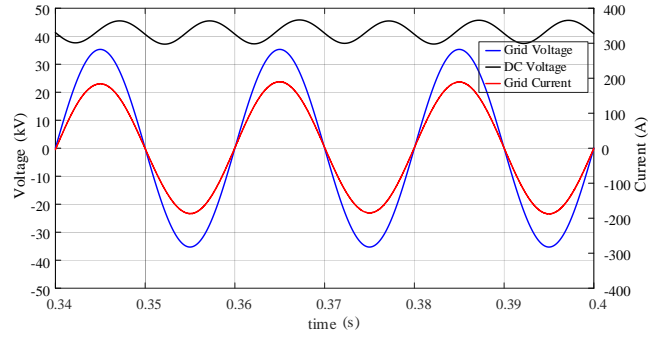


Figure 4: Simulation results of the single phase 52-level cascaded rectifier

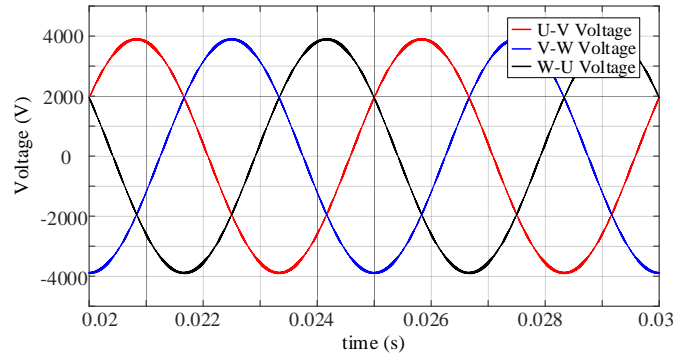


Figure 5: Simulation results of the 3 phase paralleled 2-level cascaded inverter

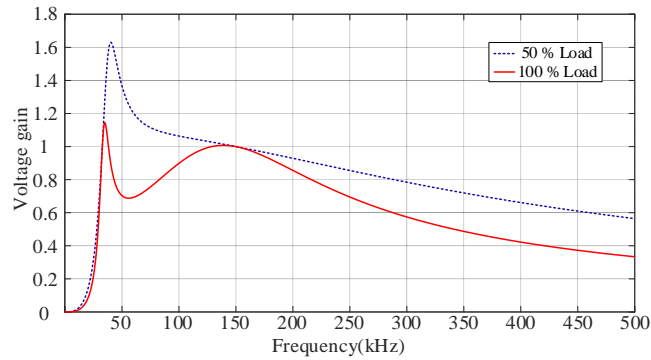


Figure 6: Voltage gain of the CLLC resonant converter under different loads

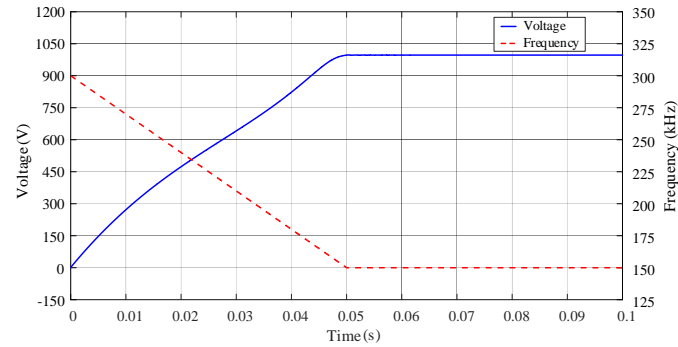


Figure 7: Simulated results of the CLLC resonant converter under soft starting strategy

## 4 Implementation Scheme Of Integrated Converter

This section first presents the loss and temperature rise results of the integrated converter using SiC devices. Then, the magnetic field distribution of the high-frequency transformer is given through simulation. Finally, a virtual prototype of the integrated converter is presented.

The integrated inverter system applies third-generation SiC devices (C3M0021120K). The front stage AC/DC of the integrated inverter system adopts a 52 stage cascade rectification scheme, the post stage DC/AC adopts a three-phase paralleled two-stage cascade inverter scheme, and the middle stage DC/DC adopts a high-frequency isolated CLLC resonance scheme. The losses and efficiency of all switching devices using three SiC devices in parallel are shown in Table 1, with a total efficiency of 98.34 %. Assuming that the integrated converter is installed in a rail vehicle with an ambient temperature of 60 °C.

	Frequency	$P_{\text{loss\_HV}}$	$P_{\text{loss\_LV}}$	Efficiency	Temperature rise
AC/DC	10 kHz	433.21 W	-	99.32 %	23.7 °C
DC/DC	150 kHz	261.69 W	93.25 W	99.43 %	9.3 °C
DC/AC	15 kHz	0	231.25 W	99.58 %	14.0 °C
$P_{\text{total}}$	-	694.90 W	324.50 W	98.34 %	-

Table 1: Power Loss and Efficiency of the Integrated Converter

Magnetic components are one of the most important passive components in power electronic systems, which can be used as energy storage components to achieve energy conversion functions, and can also be used as filter components to reduce EMI noise generated by the system. For the traction transmission and auxiliary power supply systems of rail vehicles, high-frequency and high-power magnetic components have become the key to further improving the power density and efficiency of the system [8].

High frequency isolation transformers require the use of low core loss magnetic cores, such as ferrite, amorphous alloys, nanocrystalline alloys, etc. Ferrite cores have the characteristics of low cost and low loss, making them very suitable for transformer applications in the frequency range of 20 kHz to 3 MHz. High frequency transformer excitation inductance target value 100  $\mu\text{H}$ . An air gap needs to be added to the magnetic core. Simultaneously increasing the air gap will increase the leakage flux of the transformer, leading to high leakage inductance, which will affect the resonant frequency of the resonant unit. The high-frequency transformer composed of 49925 U-shaped magnetic cores is shown in Figure 8, where the internal winding is the primary winding and the external winding is the secondary winding. This winding arrangement method can increase the coupling coefficient of the primary and secondary windings. The simulation results of magnetic flux distribution are also shown in Figure 8.

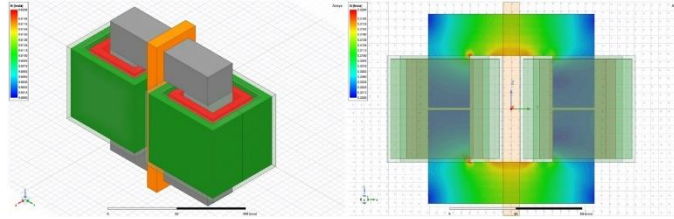


Figure 8: Leakage inductance simulation of the high frequency transformer

Air gap(mm)	Coupling coefficient	Magnetizing inductance	Primary leakage $L$	Secondary leakage $L$	Turns ration
2.56 (calculated)	0.9881	121.95 $\mu$ H	1.56 $\mu$ H	1.37 $\mu$ H	13 : 13
3.28 (optimized)	0.9857	100.01 $\mu$ H	1.54 $\mu$ H	1.36 $\mu$ H	13 : 13
4.00 (optimized)	0.9837	100.09 $\mu$ H	1.67 $\mu$ H	1.65 $\mu$ H	14

Table 2: Coupling Coefficient and Leakage Inductance Under Different Air Gaps

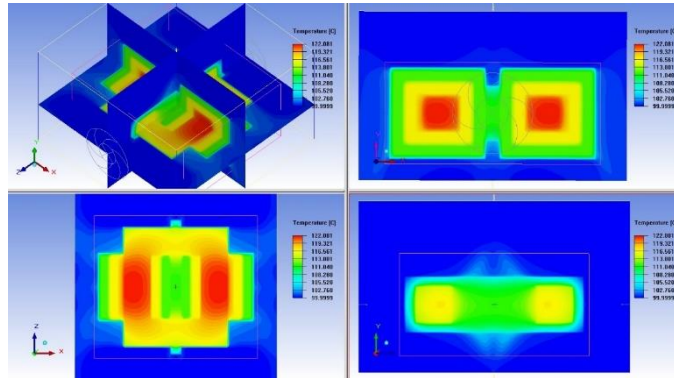


Figure 9: Temperature rise simulation of the high frequency transformer

Due to the neglect of the edge magnetic flux in the air gap calculation, the actual excitation inductance is higher than the expected value. This section simulates and analyzes the leakage inductance caused by air gaps. The simulation results of transformers designed with 49925UC magnetic cores under different air gaps are shown in Table 2.

Under forced air cooling conditions (dual cooling fans, 50 cfm), the temperature rise simulation results at an ambient temperature of 100 °C are shown in Figure 9. The highest temperature rise is 22.08 °C, and the highest temperature point is located at the ferrite core (winding wrapping).

## 5 Conclusions and Contributions

The correctness and effectiveness of the SiC based power electronic transformer and sine wave traction inverter integrated system have been proven through simulation analysis. The main conclusions are as follows: the input of the integrated converter can be directly connected to the traction network (25 kV), and the output can drive 4 traction motors and provide 4 sets of auxiliary power sources, with a total power of



3.25 MVA. When the system operates at a rated power of 3.25 MVA, the total harmonic distortion (THD) of the input current is less than 1 %, the power factor is greater than 0.99, and the output voltage THD is less than 3.50 %; The overall efficiency of the system is estimated to be greater than 97.5%, which is 3% to 5% higher than the efficiency of traditional traction transmission systems. The overall weight of the system is estimated to be 2400 kg, which is 43% lighter than traditional solutions.

## References

- [1] She X , Huang A Q , Burgos R . Review of solid-state transformer technologies and their application in power distribution systems[J] . IEEE Journal of Emerging and Selected Topics in Power Electronics, 2013, 1(3): 186-198.
- [2] Feng J H, Chu W Q, Zhang Z X, et al. Power electronic transformer-based railway traction systems: challenges and opportunities[J]. IEEE Journal of Emerging and Selected Topics in Power Electronics, 2017, 5(3): 1237-1253. Kolar J W, Ortiz G I.
- [3] Solid-state-transformers: key components of future traction and smart grid systems[C]. Proceedings of the International Power Electronics Conference. Hiroshima, Japan: IPEC, 2014 .
- [4] Qu J, Zhang Q, Yuan X, and Cui S, Design of a paralleled SiC MOSFET half-bridge unit with distributed arrangement of dc capacitors[R], IEEE Transactions on Power Electronics, 2020: 10879-10891. Chen C, Chen Y, Tan Y, Fang J, et al. On the practical design of a high power density SiC single-phase uninterrupted power supply system[R], IEEE Transactions on Industrial Informatics, 2017: 2704-2716.
- [5] Fabre J and Ladoux P. Parallel connection of 1200-V/100-A SiC-MOSFET half-bridge modules [R], IEEE Transactions on Industry Applications, 2016: 1669-1676.
- [6] Oswald N, Anthony P, McNeill N, and Stark B H, An experimental investigation of the trade off between switching losses and EMI generation with hard-switched All-Si, Si-SiC, and All-SiC device combinations[R], IEEE Transactions on Power Electronics, 2014: 2393-2407.
- [7] Zhang B and Wang S, Analysis and reduction of the near magnetic field emission from toroidal inductors[R], IEEE Transactions on Power Electronics, 2020: 6251-6268.
- [8] Jiang C, Li X, Ghosh S, et al, Nanocrystalline powder cores for high-power high-frequency power electronics applications[R], IEEE Transactions on Power Electronics, 2020: 10821-10830.